ACS Catalysis

pubs.acs.org/acscatalysis

Research Article

Rhodium-Catalyzed Asymmetric Hydroselenation of 1-Alkynylindoles for Atroposelective Synthesis of Vinyl Selenoethers

Yulong Kang, Fen Wang, and Xingwei Li*

Cite This: *ACS Catal.* 2024, 14, 13055−13064

Read Online

ACCESS | Metrics & More | Article Recommendations | Supporting Information

ABSTRACT: Catalytic asymmetric hydrofunctionalization of π-bonds has been extensively studied, but the asymmetric hydrofunctionalization of alkynes that affords atropoisomeric products remains heavily underexplored. We herein report [Rh(COD)-OAc]$_2$/Mg(NTf$_2$)$_2$-catayzed highly atroposelective hydroselenation of two classes of 1-alkynylindoles using selenophenols, where the Mg(II) salt both activates the Rh catalyst and provides a key NTf$_2$ anion essential for the catalytic activity and enantioselectivity, affording C−N axially chiral trisubstituted olefins that bear a relatively low racemization barrier ($\Delta G^{\ddagger} \sim 27$ kcal/mol). The catalytic system features high activity, mild reaction conditions, good functional group tolerance, and high regio-, (*E*)-, and enantioselectivity. The selenoether moiety in the product framework can be readily functionalized to give synthetically useful products.

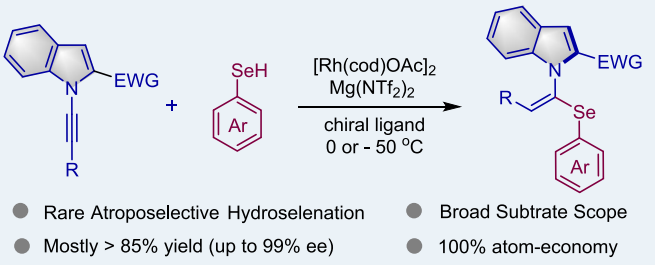

KEYWORDS: *asymmetric hydroselenation, alkyne, rhodium, selenoether, axial chirality*

INTRODUCTION

Selenium is an essential trace element in the human body, and it plays an important role in the metabolism.[1] The replacement of the lighter congeners of the chalcogen elements with selenium in natural products,[2] drug molecules,[3] and materials often significantly improved their biological activities or material properties.[4] Meanwhile, chiral selenium compounds are also widely used as catalysts in the field of asymmetric catalysis (Scheme 1A).[5b] Consequently, catalytic asymmetric synthesis of chiral organoseleniums has received increasing attention.[6] The synthesis of chiral selenoethers bears a formidable challenge in general due to the soft nature of the selenium atom that readily binds to the metal center. Besides this catalyst deactivation, the ligating ability of selenium in the substrate or the product renders it a competing ligand to interfere with the asymmetric induction, which accounts for the rarity of enantioselective hydroselenation reactions. In 2020, the Wang group demonstrated Rh(I)-catalyzed asymmetric formal hydroselenation of strained bicyclic olefins with a diselenide together with a secondary phosphine oxide.[6f] In 2022, the group of Dong and Yang reported the first enantioselective hydroselenation of styrene that proceeds through a Rh(III)-H intermediate and the reaction occurred with excellent branched-selectivity and enantioselectivity (Scheme 1B).[7] In 2024, You and co-workers reported Rh(III)-catalyzed atroposelective C−H activation-selenization of arenes using an electrophilic selenization reagent (Scheme 1B).[8] Despite this progress, a more atom-economical process such as direct hydroselenation would be ideal to prepare chiral organoseleniums. Given the limited reaction patterns and the rarity of Se-containing axially chiral products, it is desirable to develop new synthetic methods to fulfill the increasing demand of chiral organoselenium compounds.

On the other hand, with the significance of axially chiral compounds in various regimes, catalytic atroposelective synthesis has been recognized a dynamic research field.[9] Among the ample examples of axially chiral scaffolds, axially chiral olefins remain underexplored.[9e] Their synthetic challenges are largely linked to the racemization barrier of axially chiral olefins. Tetrasubstituted ones are relatively configurationally stable, while trisubstituted ones generally possess a lower racemization barrier.[10] This intrinsic property makes it more challenging to develop highly atroposelective synthetic methods when compared with axially chiral biaryls[11] or heterobiaryls[12] that have been heavily explored. Among the chiral trisubstituted olefins, the barrier is also correlated to the intrinsic properties of the substituent along the chiral axis (Scheme 1C). An aryl group, despite its small size, renders a reasonably high barrier. With the presence of a lone pair, a phosphino group gives a lower barrier. In this line, a chalcogen group defined by two lone pairs leads to an even lower barrier.

Received: June 22, 2024
Revised: August 4, 2024
Accepted: August 6, 2024

Scheme 1. Catalytic Asymmetric Synthesis of Organoseleniums and Atroposelective Hydrofunctionalization of Alkynes

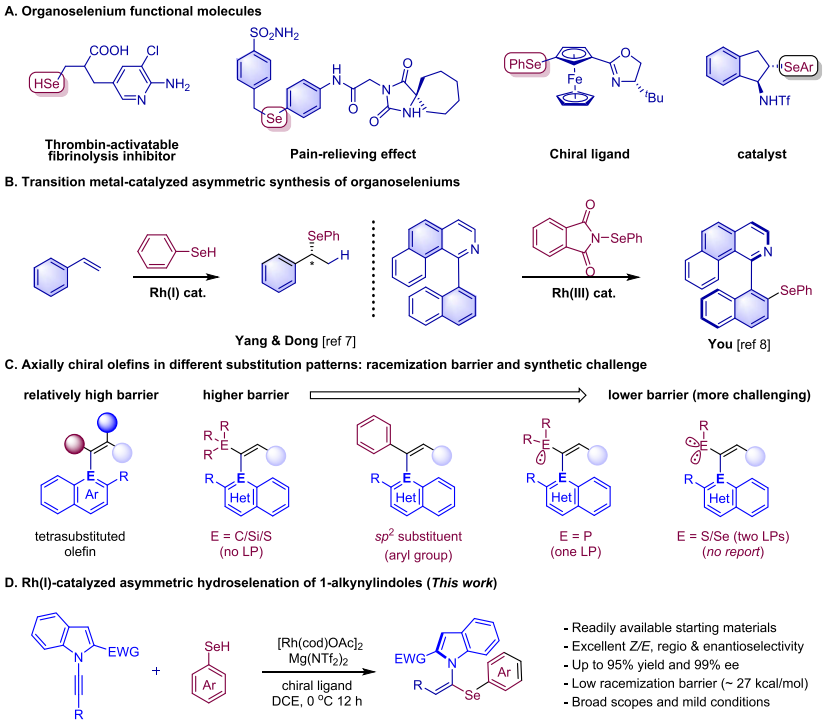

Consequently, chalcogen-functionalized axially chiral olefins have not been disclosed. Catalytic asymmetric hydrofunctionalization of alkynes offers an important solution to address this challenge.[13] In 2018, Yan reported organocatalyzed hydrosulfonylation of 1-alkynyl-2-naphthols with excellent atroposelectivity.[14] Tan and Houk elegantly realized CPA-catalyzed hydroarylation of alkynes using 2-naphthols.[15] Our group and Wang independently disclosed the hydrophosphination of sterically hindered alkynes using rhodium and copper catalysis, respectively.[16] Very recently, the Zhu group achieved Ni hydride-catalyzed asymmetric reductive hydroarylation of alkyne using aryl bromide as an aryl source.[17] The Song's group realized synthesis of axially chiral olefins via formal hydroarylation of tetracoordinate boron-functionalized internal alkyne and a sterically hindered aryl bromide, which occurs via a 1,3-nickel shift followed by deborylation.[18] The Liu group adopted an alternative approach and realized a Pd-catalyzed redox-neutral hydroarylation of 1-alkynylindole with phenylboronic acid.[19] Meanwhile, the group of Gao and Yao realized in 2023 the first Pt-catalyzed atroposelective hydrosilylation of structurally related alkynes.[20]

Although considerable progress has been made in the catalytic asymmetric hydrofunctionalization of alkynes, atroposelective hydroselenation remains unknown, likely ascribed to the low racemization barrier of the selenoether product (Scheme 1C). Inspired by the latest research in Rh-catalyzed asymmetric olefin hydroselenation,[7] we envisioned that rhodium-catalyzed asymmetric alkyne hydroselenation may be feasible. To overcome the deactivation of the catalyst caused by the selenol or the selenoether product, we adopted electron-rich chiral bidentate phosphines as ligands and used 1-alkynylindole as an electronically activated alkyne. It is worth noting that indole-based axially chiral platform represents a privileged class of functional molecules.[21] We now report $[Rh(cod)OAc]_2/Mg(NTf_2)_2$-catalyzed asymmetric hydroselenation of 1-alkyne with excellent regio-, *Z*/*E*-, and enantioselectivity (Scheme 1D).

MATERIALS AND METHODS

Materials. All chemicals were obtained from commercial sources and were used as received unless otherwise noted.

Catalytic Reactions. A borosilicate sealable tube (8 mL) was charged with 1-alkynyl-2-phosphorylindole (0.1 mmol), $[Rh(cod)OAc]_2$ (3 mol %), L (7 mol %), $Mg(NTf_2)_2$ (6 mol %), and anhydrous DCE (2.0 mL) under N_2. The resulting mixture was stirred for 10 min at 0 °C. Then, selenol 2a (0.3 mmol) was added, and the mixture was stirred at 0 °C for 12 h. The reaction mixture was concentrated under vacuum, and the residue was purified by flash chromatography using silica gel.

Initial Optimization Studies. Given the relatively small size of a SeAr group along the chiral axis in the hydroselenation product when using a 1-indolylalkyne, a suitable bulky group such as phosphoryl or sulfonyl needs to be attached to the 2-position of an indole ring to ensure atropostability. Initially, we chose 1-alkynyl-2-phosphorylindole and phenylselenol as the model substrates. It was found that the target product started to be obtained when catalyzed by $[Rh(cod)OAc]_2/Mg(NTf_2)_2$ (see the Supporting Information for details). Subsequently, a series of C_2-symmetric bidentate phosphine ligands were screened at 25 °C (Table 1). Among the ligands studied, methoxy-substituted arylphosphines generally offered good enantioselective control (**L7**, **L9**, and **L10**). Moreover, high regioselectivity and Z/E selectivity were obtained with no other regioisomers being observed. Increasing the steric hindrance of the substituents on the phosphine was beneficial to the enantioselectivity (**L2** versus **L5** and **L9** versus **L10**). When tetra-methoxy groups were introduced to the biaryl ring of the phosphine ligand, the yield was greatly improved (**L7**, **L9**, and **L10**). Finally, when a trimethylsilyl group was introduced to the 3- and 5- positions of the benzene ring of

https://doi.org/10.1021/acscatal.4c03710
ACS Catal. 2024, 14, 13055−13064

Table 1. Initial Screening of Chiral Ligands[a]

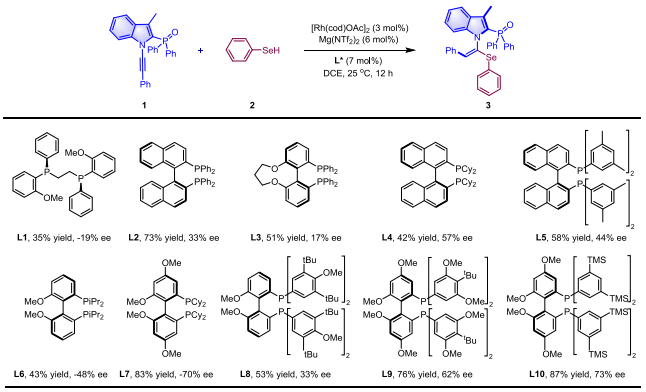

[a]Reaction conditions: $[Rh(cod)OAc]_2$ (3.0 mol %), ligand (7.0 mol %), $Mg(NTf_2)_2$ (6.0 mol %), **1** (0.1 mmol), **2** (0.12 mmol) in DCE (0.05 M) at 25 °C for 12 h under N_2; isolated yield. The ee was determined by HPLC using a chiral stationary phase.

the diphosphine ligand (**L10**), both good yield and enantioselectivity were realized. Therefore, this ligand was retained for further studies.

Further optimization studies were made using **L10** as a ligand (Table 2). DCE was established as an optimal solvent, and the reaction yield and enantioselectivity decreased when other solvents were used (entries 1−4). Subsequently, the reaction temperature was screened, and it was found that maximum enantioselectivity was attained when the reaction was conducted at 0 °C, while further lowering the temperature to −5 °C decreased the enantioselectivity (entries 5−7). After the optimal temperature was identified, the rhodium catalyst was then determined. The counteranion in the Rh(I) catalyst had drastic effects on the catalytic activity, and it was found that $[Rh(cod)OAc]_2/Mg(NTf_2)_2$ and $[Rh(cod)_2]NTf_2$ provided almost the same enantioselectivity, but the latter exhibited lower reactivity (entries 8−10, vide infra). When the amount of PhSeH was increased to 3 equiv, we were surprised to find that the enantioselectivity (97% ee) and yield (95%) had been greatly improved after 12 h (entry 11). Under otherwise the same conditions using $[Rh(cod)_2]NTf_2$ as a catalyst, the reaction time needs to be extended to 24 h to reach the same outcomes (entry 12).

Reaction Scope. With the establishment of optimal reaction conditions, we then explored the generality and limitations of this coupling system. The scope of the 1-alkynyl-2-phosphorylindole substrate was next examined (Scheme 2). Thus, the reaction was effective for substrates with a F, Cl, or Br substituent at the 5-position of the 3-methylindole ring (**4**−**6**), and both the enantioselectivity and the reaction efficiency were close to those of the parent substrate. Especially, the highest enantioselectivity (99% ee) was realized for a 5-fluoro-substituted substrate (**4**). Variation of the 3-substituent to a phenyl or an ester alkyl group also verified their compatibility, as in the isolation of products **7** and **8** in high regio-, stereo-, and enantioselectivity. The absolute configuration of product **3** has been determined by ECD spectroscopy, and the racemization barrier of product **3** was measured to be $\Delta G^{\ddagger}_{rac}$ = 27.1 kcal/mol (70 °C, DCE), which is relatively low. Additionally, a 3-unsubstituted indole also reacted effectively (product **9**, 90% yield and 96% ee). Various substituents such as methyl, methoxy, and benzyloxy in the indole ring were also compatible (**10**-**13**, 91−97% ee). It was worth noting that when the methoxy or benzyloxy groups were located at the 4-position (**11** and **12**), the enantioselectivity slightly decreased, but when the benzyloxy group was located at the 5-position (**13**), the enantioselectivity was close to that of the parent substrate. In contrast, the introduction of a F, Cl, Br, or ester group into different positions of the indole ring greatly retarded the reaction, indicative of strong electronic effect of the indole ring under the initial standard conditions. To our delight, when the **L7** ligand was used as a back-up ligand, the target product was obtained in a moderate yield in >90% ee with the opposite configuration (**15**−**18**). Extension of the alkyne terminus to a phenyl group bearing electron-rich (**19**−

Table 2. Further Optimization Studies[a,b,c]

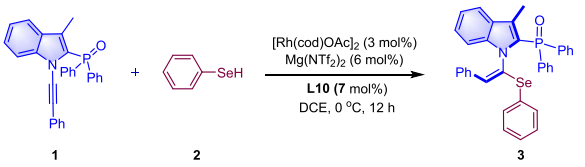

entry	catalyst	additive	solvent/T	yield (%)/Ee (%)
1	$[Rh(cod)OAc]_2$	$Mg(NTf_2)_2$	DCE/25 °C	87/73
2	$[Rh(cod)OAc]_2$	$Mg(NTf_2)_2$	DCM/25 °C	85/69
3	$[Rh(cod)OAc]_2$	$Mg(NTf_2)_2$	PhCl/25 °C	76/58
4	$[Rh(cod)OAc]_2$	$Mg(NTf_2)_2$	MTBE/25 °C	81/51
5	$[Rh(cod)OAc]_2$	$Mg(NTf_2)_2$	DCE/10 °C	81/82
6	$[Rh(cod)OAc]_2$	$Mg(NTf_2)_2$	DCE/0 °C	79/91
7	$[Rh(cod)OAc]_2$	$Mg(NTf_2)_2$	DCE/-5 °C	62/87
8	$[Rh(cod)_2]BF_4$		DCE/0 °C	N.R.
9	$[Rh(cod)_2]OTf$		DCE/0 °C	69/87
10	$[Rh(cod)_2]NTf_2$		DCE/0 °C	71/91
11[b]	$[Rh(cod)OAc]_2$	$Mg(NTf_2)_2$	DCE/0 °C	95/97
12[c]	$[Rh(cod)_2]NTf_2$		DCE/0 °C	95/97

[a]Reaction conditions: **1** (0.1 mmol), **2** (0.12 mmol), catalyst (3 mol % for dimeric catalyst or 6 mol % for monomeric catalyst), **L10** (7 mol %), and $Mg(NTf_2)_2$ (6 mol %) in a solvent (0.05 M), 12 h under N_2; isolated yield. The ee was determined by HPLC using a chiral stationary phase. [b]**2** (0.3 mmol), 12 h. [c]**2** (0.3 mmol).

https://doi.org/10.1021/acscatal.4c03710
ACS Catal. 2024, 14, 13055−13064

Scheme 2. Scope of the 1-Alkynyl-2-phosphorylindoles[a,b]

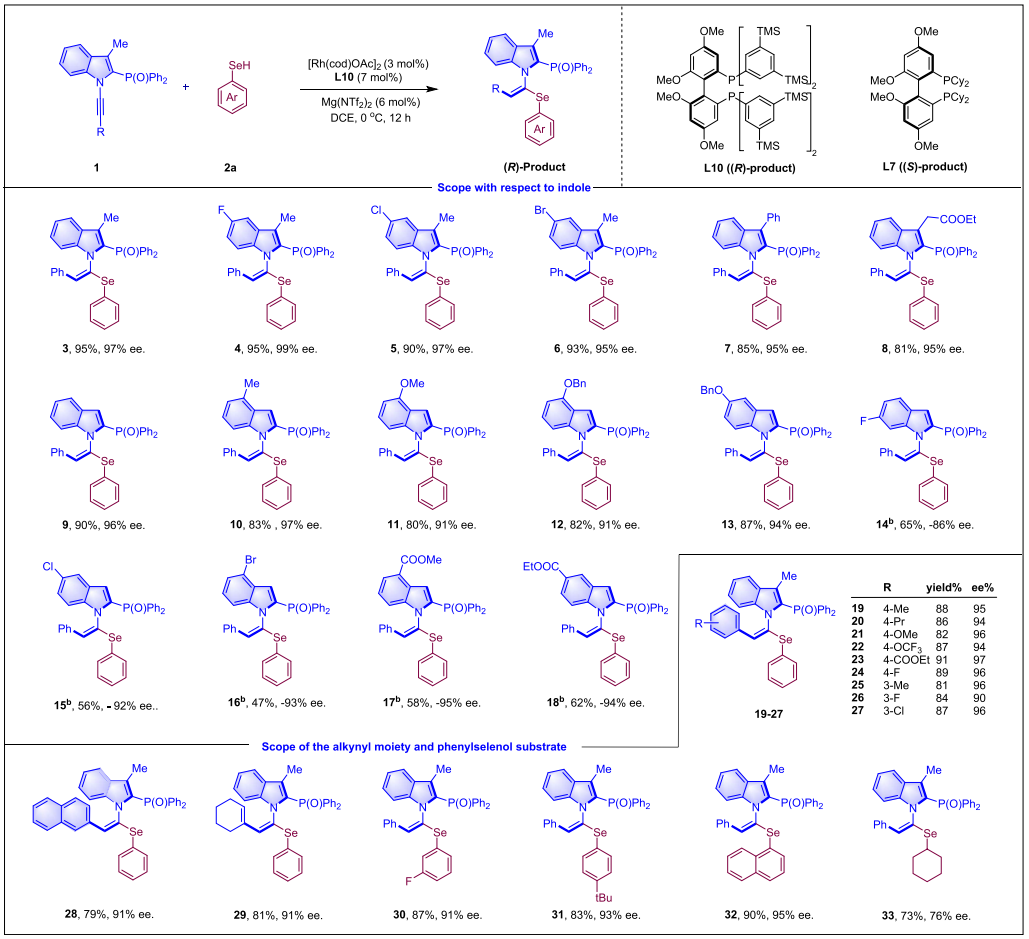

[a]Reaction conditions: $[Rh(cod)OAc]_2$ (3.0 mol %), **L10** (7.0 mol %), $Mg(NTf_2)_2$ (6.0 mol %), **1** (0.1 mmol), **2** (0.3 mmol) in DCE (0.05 M), 0 °C for 12 h under N_2; isolated yield; The ee was determined by HPLC using a chiral stationary phase. [b]**L*** = **L7**, T = 10 °C.

21 and **25**) or electron-poor (**22**−**24** and **26**−**27**) substituents at different positions only had marginal influence on the efficiency (81−91% yield) and enantioselectivity (90−97% ee) under the originally optimal conditions. The phenyl group was also successfully extended to 2-naphthyl (**28**). In addition, extension to a cyclohexenyl group was met with no difficulty, and the product was isolated in excellent enantioselectivity (**29**, 91% ee). We also briefly explored several ArSeH substrates. Similarly, electron-donating and -withdrawing substituents such 3-F and 4-^{t}Bu in the selenol had a negligible impact on enantioselectivity and regioselectivity (**30** and **31**). Similarly, the phenylselenol reagent was also extended to a more hindered 1-naphthylselenol with an excellent yield and enantioselectivity (**32**). However, when the selenol substrate was extended to cyclohexylselenol, the reaction proceeded only with a 76% ee (**33**).

To further verify the universality of the coupling system, the alkyne substrate was further expanded to 2-sulfonylindole-based alkynes with 1-naphthalnylselenol being a coupling reagent (Scheme 3). In general, the enantioselectivity of the reaction of sulfonyl-substituted alkyne is slightly lower than that of the 2-phosphoryl-substituted one, but the reactivity was much higher since the reaction took place at −50 °C. A 3-unsubstituted indole also reacted effectively in 81% yield with 90% ee (**36**). When a methyl group was introduced to the 3-, 4-, or 5-positions of the indole ring, both the enantioselectivity and the yield were maintained (**37**, **38**, and **42**). The racemization barrier of product **37** was measured to be $\Delta G^{\ddagger}_{rac}$ = 28.4 kcal/mol (80 °C, Toluene). However, when a methoxy group was introduced to the 4-, 5-, or 6-positions of the indole ring, the differences in enantioselectivity were relatively large (**40**, **43**, and **44**). The presence of a 5-chloro group in the indole ring caused a slight decrease of the enantioselectivity (**39**), and replacing the 5-Cl group with an ester then increased the enantioselectivity (**41**, 91% ee). The absolute configuration of product **44** has been confirmed by X-ray crystallographic analysis (CCDC 2359821). The electronic properties of the aryl terminus of the alkyne were also found to have a slight effect on the enantioselectivity. The introduction of fluorine, chlorine, methyl, methoxy, phenyl, and tert-butyl group into the *para* position of the benzene ring afforded the desired products in good yield and high enantioselectivity (**45**−**49**, 86−89% ee). The steric effect of the aryl group had an adverse influence on the enantioselectivity (**50**−**52**). When the aryl terminus was extended to 1-naphthyl (**53**), the enantioselectivity was greatly improved to 97% ee. Similarly, we met with no difficulty when a cyclohexenyl terminus was used (**54**, 94% ee). In addition, the reaction also showed good compatibility with cyclohexyl and cyclopropyl groups, as in the isolation of products **55** and **56** in good yields with 89−91% ee. We also attempted the reaction of 1-alkynylnaphthalene as

https://doi.org/10.1021/acscatal.4c03710
ACS Catal. 2024, 14, 13055−13064

Scheme 3. Scope of the 2-Sulfonylindole Alkyne[a]

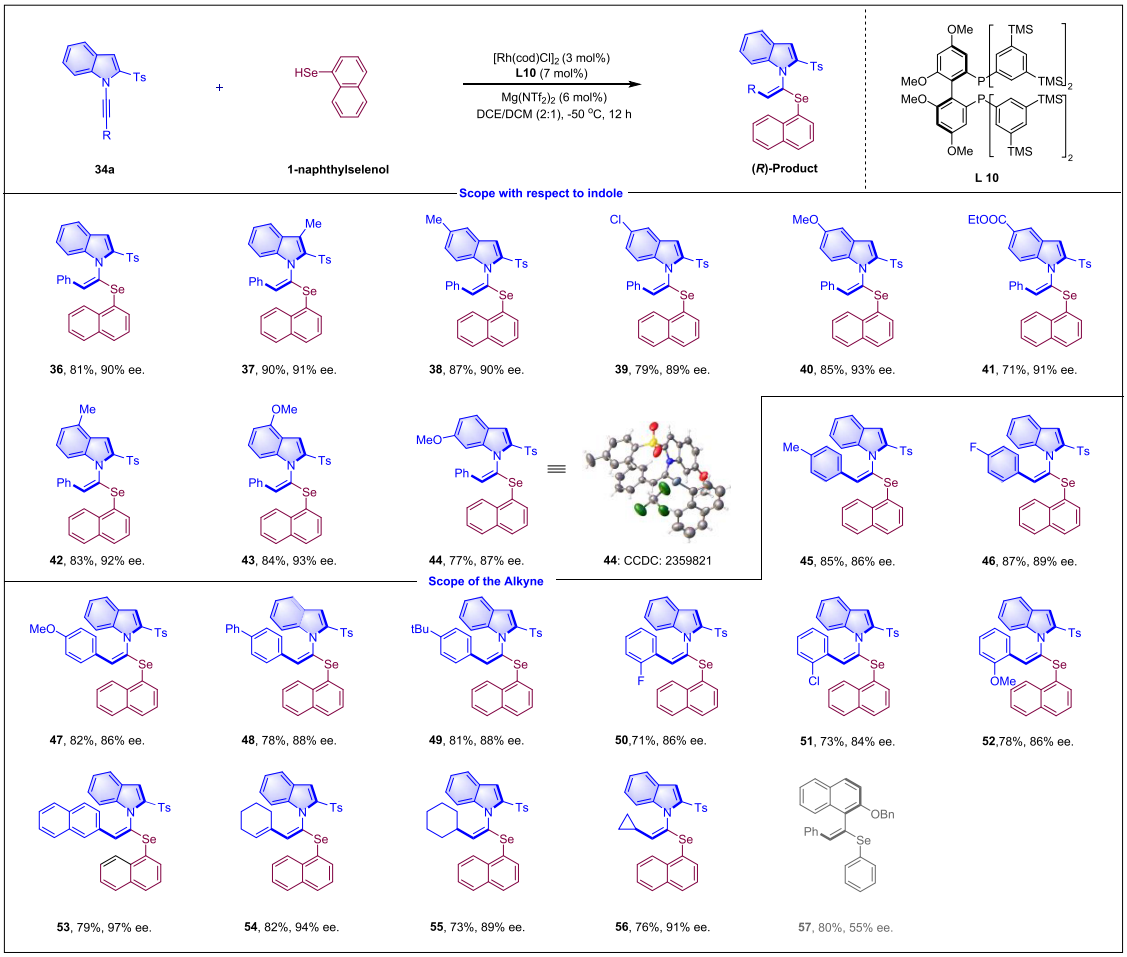

[a]Reaction conditions: $[Rh(cod)Cl]_2$ (3.0 mol %), **L10** (7.0 mol %), $Mg(NTf_2)_2$ (6.0 mol %), **1** (0.1 mmol), ArSeH (0.15 mmol) in DCE/DCM (2:1 v/v, 0.05 M) at −50 °C for 12 h under N_2; isolated yield. The ee was determined by HPLC using a chiral stationary phase.

another class of alkyne (product **57**), but the reaction proceeded with only 55% ee.

Synthetic Applications. Synthetic transformations of a representative product were performed to demonstrate the value of our protocol (Scheme 4). The reaction of 1-alkynyl-2-phosphorylindole and phenylselenol or 1-naphthylselenol was smoothly scaled up to a 1 mmol scale with no loss of enantioselectivity (Scheme 4A). The selenium in the product was easily oxidized to a selenium oxide by *m*-CPBA with excellent (>20:1) diastereoselectivity, and the enantioselectivity was also maintained (**58**). The phosphoryl group in product **32** was reduced to diphenylphosphine (**59**) under mild conditions. Subsequently, the reduced product **59** can be smoothly converted to a phosphine sulfide upon treatment with S_8 (**60**). The double bond in product **32** is electronically activated. Initially, we envisioned the use of Br_2 or NBS to realize electrophilic olefinic CH bromination. However, a substitution reaction occurred at the aryl selenium site with the silver salt as a scavenger of the SeAr group. Fortunately, the optical purity of **61** was maintained during this deselenylated bromination. The retention of the configuration is ascribed to the mild reaction conditions, and a bromonium ion is formed during the reaction, followed by the departure of the ArSe group. The introduction of a bromo group to the alkenyl position allows for diversified conversions. Thus, **61** underwent Kumada coupling with phenyl magnesium bromide under nickel catalysis to obtain **62** with a slight decrease of the enantiopurity (90% ee). Subsequently, a potential monodentate phosphine ligand was obtained by a simple reduction (**63**, 90% ee). In addition, Ni-catalyzed Stille coupling of **61** with an organic zinc reagent afforded **64** with a similar enantiopurity (91% ee). Treatment of $PdCl_2(MeCN)_2$ with **59** afforded a P−Se bidentate Pd(II) complex (**65**) in a high yield, which indicates that **59** has sufficient ligating ability as a Se−P bidentate ligand. Phosphine **63** was then designated as a chiral ligand in palladium-catalyzed asymmetric allylic alkylation, affording product **68** in 61% ee.

Mechanistic Studies. A series of experimental studies have been conducted to probe the mechanism of the coupling of alkyne **1** and PhSeH **2** (Scheme 5). First, deuterium labeling experiments were studied (Scheme 5A). The reaction of 1-alkynylindole **1** and PhSeD was carried out to give the product in 93% yield, with deuterium (85% D) incorporation at the olefinic carbon as indicated by ^1H NMR analyses. It was observed that the product had a higher deuteration level at the initial stage of the reaction (91% D, after 2h). This suggests that as the reaction proceeded, the adventitious water may participate to contribute to the C−H bond formation. Subsequently, we used PhSeH in the presence of D_2O (5 equiv) to perform the reaction. After the reaction was

https://doi.org/10.1021/acscatal.4c03710
ACS Catal. 2024, 14, 13055−13064

Scheme 4. Synthetic Applications

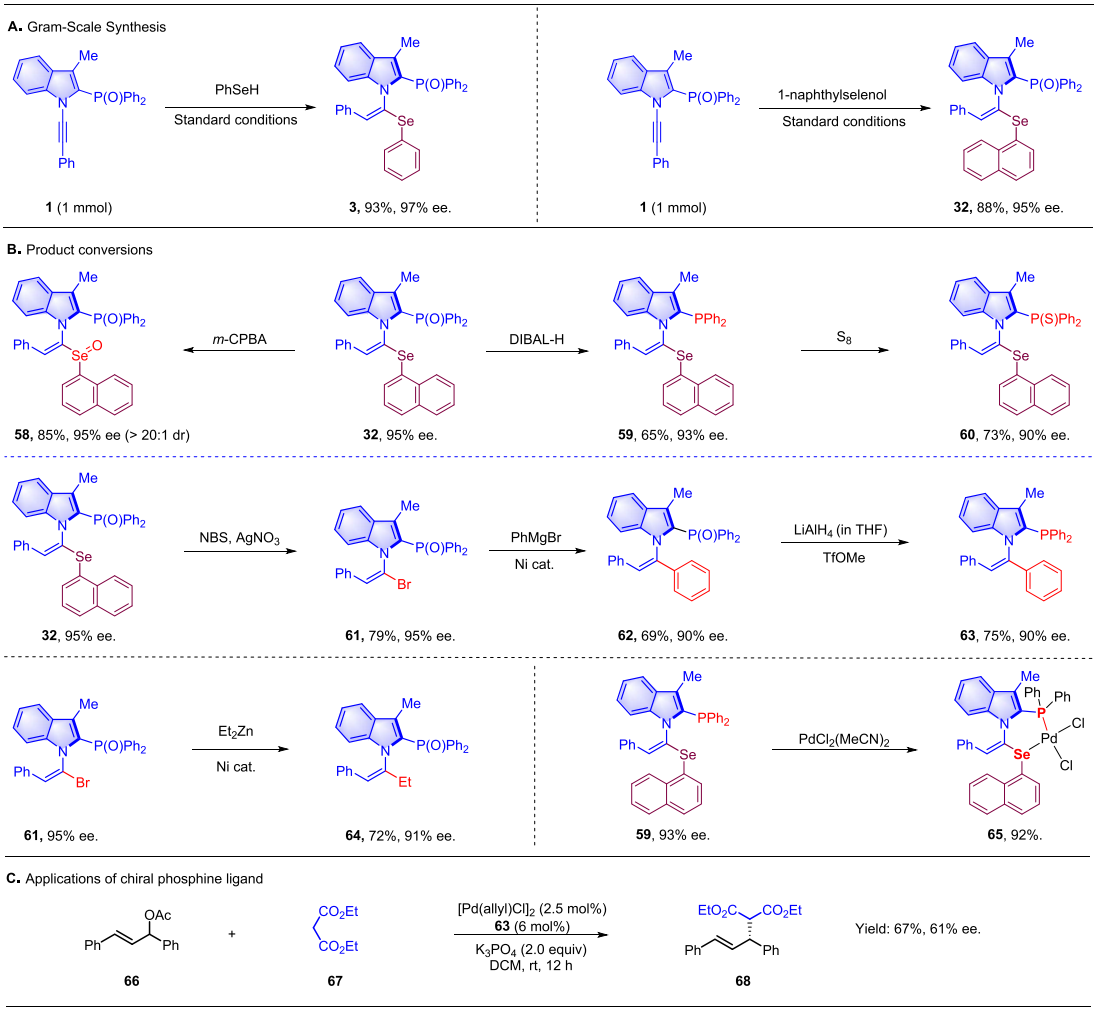

completed, the product was found to be 40% deuterated at the same position, which may be caused by the initial hydrogen−deuterium exchange between PhSeH and D_2O (Scheme 5B). Based on literature precedence,[7] we speculated that the PhSeH may undergo an oxidative addition to Rh(I) to produce a Rh(III)−H intermediate. To obtain experimental evidence, we carried out a series of studies (Scheme 5C). After mixing PhSeH, $[Rh(cod)OAc]_2$ (3 mol %), $Mg(NTf_2)_2$ (6 mol %), and **L10** (7 mol %), a broad resonance signal (δ −12.19), although weak, was observed in ^1H NMR spectroscopy within less than 10 min. Upon the addition of alkyne **1**, the hydride signal disappeared, which is in line with the proposed mechanism of Rh−H migratory insertion into olefins in Yang and Dong's studies.[7] We also determined the KIE of the reaction through two parallel initial rate studies under rigorously dry conditions, and the small value of k_H/k_D = 1.4 suggested that Se−H cleavage was not involved in the enantiodetermining step (Scheme 5D).

Next, we studied the nonlinear effect of chiral ligand **L10** (Scheme 5E). The enantiomeric purity of the chiral ligand **L10** showed a linear relationship with the enantioselectivity, indicating a 1:1 ratio between Rh(I) and the **L10** ligand in the enantiomeric determination step. The role of the Mg salt was also investigated. Under the standard reaction conditions, different amounts of $Mg(NTf_2)_2$ (3, 6, and 9 mol %) were added. The highest enantioselectivity was observed when Rh and Mg were in a 1:1 ratio. In addition, the reaction did not occur without the $Mg(NTf_2)_2$ additive (Scheme 5F). In our reaction optimization studies, $Rh(cod)_2NTf_2$ could be used alone to give the product in the same yield and enantioselectivity, although the reaction rate was lower. Then we measured the KIE (k_H/k_D = 1.6) under the reaction conditions of $Rh(cod)_2NTf_2$ and **L10**, and this value is consistent with our previous measurements. At the same time, there was an induction period for the reaction catalyzed by $Rh(cod)_2NTf_2$ alone, during which time almost no product was observed. After 30 min, the reaction rate was significantly improved (see Supporting Information for details). This indicates that the coordination of the ligand to the catalyst to give the active species is relatively slow when the $Rh(cod)_2NTf_2$ was used alone. In contrast, in the case of the $[Rh(cod)OAc]_2$-Mg(II) catalyst system, the active catalyst was rapidly generated, possibly due to a more facile substitution of the COD ligand because of the 1:1 ratio of Rh:COD. We also investigated the effects of some magnesium salts and other metal salts of NTf_2 on the reaction (See Supporting Information for details). When magnesium salts of other anions are used, such as OAc^-, SO_4^{2-}, OTf^-, and NO_3^-, the reaction does not occur. This indicates that the NTf_2 anion is indispensable in the reaction. When using different NTf_2 salts, the reaction can proceed smoothly with only $Zn(NTf_2)_2$ or $LiNTf_2$ as additives. However, the former has no enantiose-

https://doi.org/10.1021/acscatal.4c03710
ACS Catal. 2024, 14, 13055−13064

Scheme 5. Mechanistic Studies

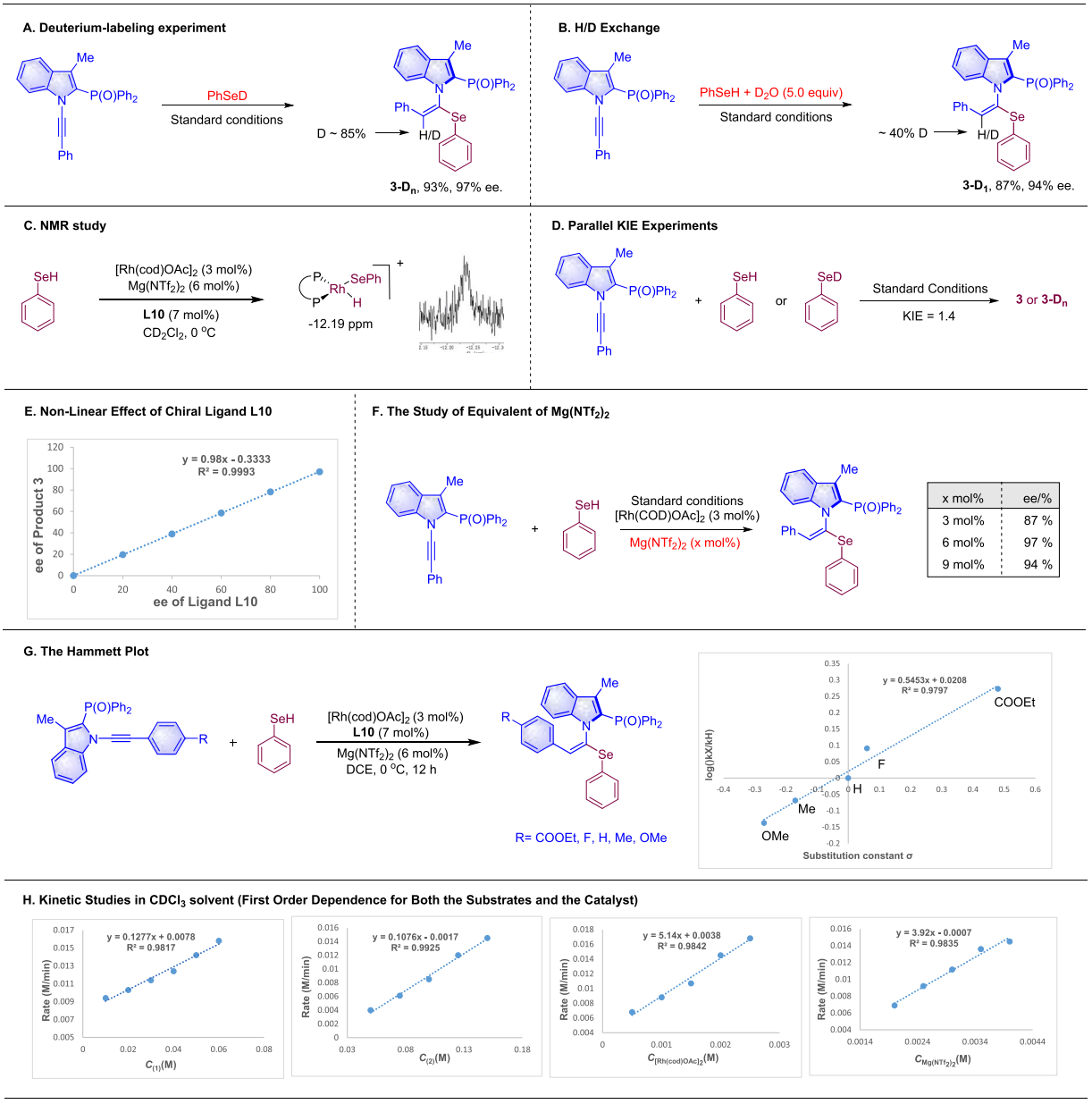

lectivity, and the latter has only 51% ee. It indicates that cations have a great influence on the reaction. Based on the above reasons, it can be concluded that both magnesium ions and NTf_2 ions have a great influence on the reaction. In order to explore the details of the mechanism, alkynes with different *para* substituents were used for a Hammett plot (Scheme 5G). A linear correlation was observed with a positive $\rho = 0.54$. This outcome suggests accumulation of negative charge in the transition state, and this seems consistent with alkyne insertion occurring prior to or during the rate-limiting step because a more electronically biased alkyne should give higher reactivity. In addition, the initial rate method was used to study the reaction kinetics (Scheme 5H), which showed that the alkyne, PhSeH, $Rh(COD)OAc]_2$, and $Mg(NTf_2)_2$ all showed first-order dependence in this coupling reaction, suggesting that all of these species contributed during the rate-limiting step.

Based on mechanistic research experiments and previous reports, a possible mechanism was proposed (Scheme 6). An active Rh catalyst is initially formed from the precatalyst $Rh(cod)OAc]_2$ and **L10** with the assistance of the $Mg(NTf_2)_2$ salt. Then, Rh(III) hydride **INT I** is obtained upon oxidative addition of the H−Se bond. The alkyne unit of substrate **1** then coordinates to **INT I** to produce **INT II**. Subsequently, the Rh−Se bond undergoes migratory insertion into the alkyne to give **INT III** with a single regioselectivity. In this insertion, the Rh ends up germinal to the small phenyl group for both electronic and steric reasons, and the other regioselectivity is unlikely due to both electronic and steric reasons.[16a,19,22] Subsequent C−H reductive elimination of **INT III** then generates the hydroselenation product, together with the active rhodium catalyst (Route A). Based on our kinetic studies, it is possible that the alkyne insertion is the rate-limiting step because this process involves the selenol, the alkyne, and the Rh catalyst. It is less likely that Rh−H reductive elimination is rate-limiting because an EWG group in the phenyl ring should disfavor the reductive elimination. We also considered the

https://doi.org/10.1021/acscatal.4c03710
ACS Catal. 2024, 14, 13055−13064

Scheme 6. Proposed Catalytic Cycle

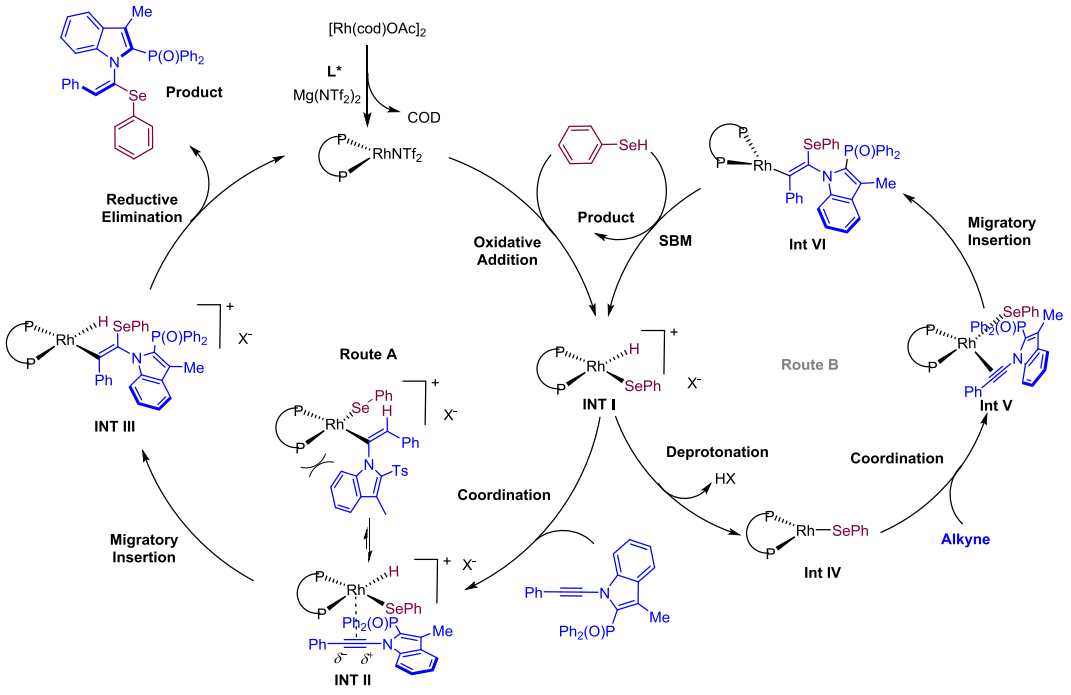

possibility of a Rh(I) cycle in which the **INT I** is deprotonated to give a Rh(I) selenide (**INT IV**) that participates in alkyne insertion (Route B). On the basis of the strong anion effect observed in our optimization studies (Table 2), the Rh(III) mechanism seems more likely due to the high oxidation state and, consequently, stronger ion-paring effects. In addition, in the case of $Rh(cod)_2NTf_2$ that worked nearly equally well, the deprotonation of Rh(III)-hydrides is less likely in the absence of any obvious base.

CONCLUSIONS

In summary, we have developed a rhodium-catalyzed asymmetric hydroselenation of two closely related classes of sterically hindered alkynes using readily available selenophenols, providing C−N axially chiral trisubstituted selenoethers that bear a relatively low barrier of racemization. The coupling reaction proceeded with excellent regioselectivity, *E*-selectivity, and enantioselectivity under mild conditions. The catalytic system utilizes a combination of $[Rh(cod)OAc]_2$ and $Mg(NTf_2)_2$, where the Mg(II) salt both activates the Rh catalyst and provides a key NTf_2 anion necessary for the reaction system, which greatly improves the catalytic reactivity. In addition, selected chiral products have been shown to be useful ligands in metal-catalyzed asymmetric reactions. Owing to the wide applications of indoles and organoselenium compounds in diverse fields, we hope that the reaction may find important implications toward further asymmetric construction of related functional molecules.

ASSOCIATED CONTENT

Supporting Information

The Supporting Information is available free of charge at https://pubs.acs.org/doi/10.1021/acscatal.4c03710.

Detailed experimental procedures, characterization data, X-ray crystallographic data for **44**, and NMR spectra of new compounds (PDF)

Accession Codes

CCDC 2359821 contain the supplementary crystallographic data for this paper. These data can be obtained free of charge via www.ccdc.cam.ac.uk/data_request/cif, or by emailing data_request@ccdc.cam.ac.uk, or by contacting The Cambridge Crystallographic Data Centre, 12 Union Road, Cambridge CB2 1EZ, UK; fax: + 44 1223 336033.

AUTHOR INFORMATION

Corresponding Author

Xingwei Li − *School of Chemistry and Chemical Engineering, Shaanxi Normal University, Xi'an 710062, P. R. China; Institute of Frontier Chemistry, School of Chemistry and Chemical Engineering, Shandong University, Qingdao 266237, P. R. China;* orcid.org/0000-0002-1153-1558; Email: lixw@snnu.edu.cn

Authors

Yulong Kang − *School of Chemistry and Chemical Engineering, Shaanxi Normal University, Xi'an 710062, P. R. China*

Fen Wang − *School of Chemistry and Chemical Engineering, Shaanxi Normal University, Xi'an 710062, P. R. China*

Complete contact information is available at: https://pubs.acs.org/10.1021/acscatal.4c03710

Notes

The authors declare no competing financial interest.

ACKNOWLEDGMENTS

Financial support from the NSFC (Nos. 22371175 and 22101167) and from the Central Universities of China (GK202306002) is gratefully acknowledged. The authors thank Prof. Xiao-Hui Yang for helpful discussions.

REFERENCES

(1) (a) Labunskyy, V. M.; Hatfield, D. L.; Gladyshev, V. N. Selenoproteins: Molecular Pathways and Physiological. *Roles. Physiol. Rev.* **2014**, *94*, 739−777. (b) Rayman, M. P. Selenium and Human Health. *Lancet* **2012**, *379*, 1256−1268. (c) Rayman, M. P. The Importance of Selenium to Human Health. *Lancet* **2000**, *356*, 233−241.

(2) (a) Cheng, K.; Sun, Y.; Liu, B.; Ming, J.; Wang, L.; Xu, C.; Xiao, Y.; Zhang, C.; Shang, L. Selenium Modification of Natural Products and Its Research Progress. *Foods* **2023**, *12*, 3773. (b) Chen, X.; Li, B. How Nature Incorporates Sulfur and Selenium into Bioactive Natural Products. *Curr. Opin. Chem. Biol.* **2023**, *76*, No. 102377. (c) Hou, W.; Dong, H.; Zhang, X.; Wang, Y.; Su, L.; Xu, H. Selenium as an Emerging Versatile Player in Heterocycles and Natural Products Modification. *Drug Discovery Today* **2022**, *27*, 2268−2277. (d) Hou, W.; Xu, H. Incorporating Selenium into Heterocycles and Natural Products-from Chemical Properties to Pharmacological Activities. *J. Med. Chem.* **2022**, *65*, 4436−4456.

(3) (a) Angelone, T.; Rocca, C.; Lionetti, V.; Penna, C.; Pagliaro, P. Expanding the Frontiers of Guardian Antioxidant Selenoproteins in Cardiovascular Pathophysiology. *Antioxid. Redox Sign.* **2024**, *40*, 369−432. (b) Huwiler, V.; Maissen-Abgottspon, S.; Stanga, Z.; Müehlebach, S.; Trepp, R.; Bally, L.; Bano, A. Selenium Supplementation in Patients with Hashimoto Thyroiditis: a Systematic Review and Meta-Analysis of Randomized Clinical Trials. *Thyroid* **2024**, *34*, 295−313. (c) Jain, V. K.; Priyadarsini, K. I. Selenium Compounds as Promising Antiviral Agents. *New J. Chem.* **2024**, *48*, 6534−6552. (d) Radomska, D.; Czarnomysy, R.; Radomski, D.; Bielawski, K. Selenium Compounds as Novel Potential Anticancer Agents. *J. Mol. Sci.* **2021**, *22*, 1009−1035. (e) Ali, W.; Benedetti, R.; Handzlik, J.; Zwergel, C.; Battistelli, C. The Innovative Potential of Selenium-Containing Agents for Fighting Cancer and Viral Infections. *Drug Discovery Today* **2021**, *26*, 256−263.

(4) (a) Gorska, S.; Maksymiuk, A.; Turlo, J. Selenium-Containing Polysaccharides Structural Diversity, Biosynthesis, Chemical Modifications and Biological Activity. *Appl. Sci.* **2021**, *11*, 3717. (b) Li, J.; Shen, B.; Nie, S.; Duan, Z.; Chen, K. A Combination of Selenium and Polysaccharides: Promising Therapeutic Potential. *Carbohyd. Polym.* **2019**, *206*, 163−173. (c) Shi, Z.; Zhang, H.; Khan, K.; Cao, R.; Xu, K.; Zhang, H. Two-Dimensional Selenium and Its Composites for Device Applications. *Nano. Res.* **2022**, *15*, 104−122. (d) Wadhwani, S. A.; Shedbalkar, U.; Singh, R.; Chopade, B. A. Biogenic Selenium Nanoparticles: Current Status and Future Prospects. *Appl. Microbiol. Biot.* **2016**, *100*, 2555−2566. (e) Cao, W.; Wang, L.; Xu, H. Selenium/Tellurium Containing Polymer Materials in Nanobiotechnology. *Nano. Today* **2015**, *10*, 717−736.

(5) For reviews on chiral organoselenide catalysts, see: (a) Lai, S.; Liang, X.; Zeng, Q. Recent Progress in Synthesis and Application of Chiral Organoselenium Compounds. *Chem.—Eur. J.* **2024**, *30*, No. e202304067. (b) Nishiyori, R.; Mori, T.; Okuno, K.; Shirakawa, S. Chiral Sulfide and Selenide Catalysts for Asymmetric Halocyclizations and Related Reactions. *Org. Biomol. Chem.* **2023**, *21*, 3263−3275. (c) Liao, L.; Zhao, X. Indane-Based Chiral Aryl Chalcogenide Catalysts: Development and Applications in Asymmetric Electrophilic Reactions. *Acc. Chem. Res.* **2022**, *55*, 2439−2453. For select recent examples, see: (d) Qi, Z.; Li, Y.; Wang, J.; Ma, L.; Wang, G.-W.; Yang, S.-D. Electrophilic Selenium-Catalyzed Desymmetrizing Cyclization to Access P-Stereogenic Heterocycles. *ACS Catal.* **2023**, *13*, 13301−13309. (e) Luo, H.-Y.; Li, Z.-H.; Zhu, D.; Yang, Q.; Cao, R.-F.; Ding, T.-M.; Chen, Z.-M. Chiral Selenide/Achiral Sulfonic Acid Cocatalyzed Atroposelective Sulfenylation of Biaryl Phenols via a Desymmetrization/Kinetic Resolution Sequence. *J. Am. Chem. Soc.* **2022**, *144*, 2943−2952. (f) Nishiyori, R.; Okuno, K.; Chan, B.; Shirakawa, S. Chiral Bifunctional Selenide Catalysts for Asymmetric Iodolactonizations. *Chem. Pharm. Bull.* **2022**, *70*, 599−604. (g) Wang, Q.; Nilsson, T.; Eriksson, L.; Szabó, K. J. Sulfenofunctionalization of Chiral α-Trifluoromethyl Allylboronic Acids: Asymmetric Synthesis of SCF_3, SCF_2R, SCN and SAr Compounds. *Angew. Chem., Int. Ed.* **2022**, *61*, No. e202210509. (h) Zhang, Y.; Liang, Y.; Zhao, X. Chiral Selenide-Catalyzed, Highly Regio- and Enantioselective Intermolecular Thioarylation of Alkenes with Phenols. *ACS Catal.* **2021**, *11*, 3755−3761. (i) Guo, R.; Liu, Z.; Zhao, X. Efficient Synthesis of P-Chirogenic Compounds Enabled by Chiral Selenide-Catalyzed Enantioselective Electrophilic Aromatic Halogenation. *CCS Chem.* **2021**, *3*, 2617−2628. (j) Nishiyori, R.; Maynard, J. J.; Shirakawa, S. Chiral Bifunctional Selenide Catalysts for Asymmetric Bromolactonization. *Asian J. Org. Chem.* **2020**, *9*, 192−196.

(6) (a) Stadel, J. T.; Back, T. G. Asymmetric Synthesis with Organoselenium Compounds-The Past Twelve Years. *Chem.—Eur. J.* **2024**, *30*, No. e202304074. (b) Chen, L. L.; Cao, R. F.; Ke, H.; Chen, Z. M. Lewis Base Catalyzed Selenofunctionalization of Alkynes with Acid-Controlled Divergent Chemoselectivity. *Chin. J. Chem.* **2024**, *42*, 1623−1629. (c) Tian, H.; Zhang, H.-M.; Yin, L. Copper(I)-Catalyzed Conjugate Addition/Enantioselective Protonation with Selenols and α-Substituted α, β-Unsaturated Thioamides. *Angew. Chem., Int. Ed.* **2023**, *62*, No. e202301422. (d) You, X.-Y.; Cai, Q. Catalytic Enantioselective Inverse-Electron-Demand Diels-Alder Reaction of 2-Pyrones and Vinyl Selenides. *Synlett* **2023**, *34*, 948−952. (e) Cao, R. F.; Yu, L.; Huo, Y. X.; Li, Y.; Xue, X. S.; Chen, Z. M. Chiral Lewis Base Catalyzed Enantioselective Selenocyclization of 1,1-Disubstituted Alkenes: Asymmetric Synthesis of Selenium-Containing 4H-3,1-Benzoxazines. *Org. Lett.* **2022**, *24*, 4093−4098. (f) Li, E.; Chen, J.; Huang, Y. Enantioselective Seleno-Michael Addition Reactions Catalyzed by a Chiral Bifunctional N-Heterocyclic Carbene with Noncovalent Activation. *Angew. Chem., Int. Ed.* **2022**, *61*, No. e202202040. (g) Lin, X.; Tan, Z.; Yang, W.; Liu, X.; Feng, X. M. Chiral Cobalt (II) Complex Catalyzed Asymmetric [2,3]-Sigmatropic Rearrangement of Allylic Selenides With α-Diazo Pyrazoleamides. *CCS Chem.* **2021**, *3*, 1423−1433. (h) Li, S.; Yang, Q.; Bian, Z.; Wang, J. Rhodium-Catalyzed Enantioselective Hydroselenation of Heterobicyclic Alkenes. *Org. Lett.* **2020**, *22*, 2781−2785. (i) Wu, D.; Qiu, J. S.; Li, C. Q.; Yuan, L. X.; Yin, H. Q.; Chen, F. X. Lewis Acid-Catalyzed Asymmetric Selenocyanation of β-Ketoesters with N-Selenocyanatosaccharin. *J. Org. Chem.* **2020**, *85*, 934−941. (j) See, J. Y.; Yang, H.; Zhao, Y.; Wong, M. W.; Ke, Z. H.; Yeung, Y. Y. Desymmetrizing Enantio- and Diastereoselective Selenoetherification through Supramolecular Catalysis. *ACS Catal.* **2018**, *8*, 850−858. (k) Zhang, H.; Lin, S.; Jacobsen, E. N. Enantioselective Selenocyclization via Dynamic Kinetic Resolution of Seleniranium Ions by Hydrogen-Bond Donor Catalysts. *J. Am. Chem. Soc.* **2014**, *136*, 16485−16488. (l) Denmark, S. E.; Kalyani, D.; Collins, W. R. Preparative and Mechanistic Studies toward the Rational Development of Catalytic, Enantioselective Selenoetherification Reactions. *J. Am. Chem. Soc.* **2010**, *132*, 15752−15765.

(7) Slocumb, H. S.; Nie, S. V.; Dong, M.; Yang, X.-H. Enantioselective Selenol-Ene using Rh-Hydride Catalysis. *J. Am. Chem. Soc.* **2022**, *144*, 18246−18250.

(8) Zheng, D.-S.; Xie, P.-P.; Zhao, F.; Zheng, C.; Gu, Q.; You, S.-L. Rh (III)-Catalyzed Atroposelective C−H Selenylation of 1-Aryl Isoquinolines. *ACS Catal.* **2024**, *14*, 6009−6015.

(9) For selected reviews, see: (a) Hao, Y.; Li, Z.-H.; Ma, Z.-G.; Liu, R.-X.; Ge, R.-T.; Li, Q.-Z.; Ding, T.-M.; Zhang, S.-Y. Axially Chiral Styrene-Based Organocatalysts and Their Application in Asymmetric Cascade Michael/Cyclization Reaction. *Chem. Sci.* **2023**, *14*, 9496−9502. (b) Bai, X.-F.; Cui, Y.-M.; Cao, J.; Xu, L.-W. Atropisomers with Axial and Point Chirality: Synthesis and Applications. *Acc. Chem. Res.* **2022**, *55*, 2545−2561. (c) Yue, Q.; Liu, B.; Liao, G.; Shi, B.-F. Binaphthyl Scaffold: a Class of Versatile Structure in Asymmetric C−H Functionalization. *ACS Catal.* **2022**, *12*, 9359. (d) Mei, G.-J.; Koay, W. L.; Guan, C.-Y.; Lu, Y. Atropisomers Beyond the C−C Axial Chirality: Advances in Catalytic Asymmetric Synthesis. *Chem.* **2022**, *8*, 1855−1893. (e) Wu, S.; Xiang, S.-H.; Cheng, J.-K.; Tan, B. Axially Chiral Alkenes: Atroposelective Synthesis and Applications. *Tetrahedron Chem.* **2022**, *1*, No. 100009. (f) Cheng, J. K.; Xiang, S.-H.; Li, S.; Ye, L.; Tan, B. Recent Advances in Catalytic Asymmetric Construction of Atropisomers. *Chem. Rev.* **2021**, *121*, 4805−4902.

https://doi.org/10.1021/acscatal.4c03710
ACS Catal. 2024, 14, 13055−13064

(10) For selected, see: (a) Feng, J.; Gu, Z. Atropisomerism in Styrene: Synthesis, Stability, and Applications. *SynOpen* **2021**, *5*, 68−85. (b) Qian, P.-F.; Zhou, T.; Shi, B.-F. Transition-Metal-Catalyzed Atroposelective Synthesis of Axially Chiral Styrenes. *Chem. Commun.* **2023**, *59*, 12669−12684. (c) Li, Z.-H.; Li, Q.-Z.; Bai, H.-Y.; Zhang, S.-Y. Synthetic Strategies and Mechanistic Studies of Axially Chiral Styrenes. *Chem. Catal.* **2023**, *3*, No. 100594. (d) Zhang, H.-H.; Shi, F. Organocatalytic Atroposelective Synthesis of Indole Derivatives Bearing Axial Chirality: Strategies and Applications. *Acc. Chem. Res.* **2022**, *55*, 2562−2580. (e) Wang, W.; Jiang, M. W.; Li, J. W.; Wang, F.; Li, X. J.; Zhao, J.; Li, X. W. Intermolecular Buchwald−Hartwig Reactions for Enantioselective Synthesis of Diverse Atropisomers: Rerouting the C−N Forming Mechanism to Substrate Oxygen-Assisted Reductive Elimination. *J. Am. Chem. Soc.* **2024**, *146*, 16567−16580.

(11) For selected reviews, see: (a) Xiang, S. H.; Ding, W. Y.; Wang, Y. B.; Tan, B. Catalytic Atroposelective Synthesis. *Nat. Catal.* **2024**, *7*, 483−498. (b) Chen, Y.-B.; Yang, Y.-N.; Huo, X.-Z.; Ye, L.-W.; Zhou, B. Recent Advances in the Construction of Axially Chiral Arylpyrroles. *Sci. China Chem.* **2023**, *66*, 2480−2491. (c) Bao, X.; Rodriguez, J.; Bonne, D. Enantioselective Synthesis of Atropisomers with Multiple Stereogenic Axes. *Angew. Chem., Int. Ed.* **2020**, *59*, 12623−12634. (d) Zhang, H.-H.; Li, T.-Z.; Liu, S.-J.; Shi, F. Catalytic Asymmetric Synthesis of Atropisomers Bearing Multiple Chiral Elements: an Emerging Field. *Angew. Chem., Int. Ed.* **2023**, *63*, No. e202311053.

(12) For selected reviews, see: (a) Feng, J.; Liu, R.-R. Catalytic Asymmetric Synthesis of N−N Biaryl Atropisomers. *Chem.—Eur. J.* **2024**, *30*, No. e202303165. (b) Cao, R.-F.; Chen, Z.-M. Catalytic Asymmetric Synthesis of Sulfur-Containing Atropisomers by C−S Bond Formations. *Sci. China Chem.* **2023**, *66*, 3331−3346. (c) Feng, J.; Lu, C.-J.; Liu, R.-R. Catalytic Asymmetric Synthesis of Atropisomers Featuring an Aza Axis. *Acc. Chem. Res.* **2023**, *56*, 2537−2554. (d) Cheng, J. K.; Tan, B. Chiral Phosphoric Acid-Catalyzed Enantioselective Synthesis of Axially Chiral Compounds Involving Indole Derivatives. *Chem. Rec.* **2023**, *23*, No. e202300147. (e) Centonze, G.; Portolani, C.; Righi, P.; Bencivenni, G. Enantioselective Strategies for the Synthesis Of N−N Atropisomers. *Angew. Chem., Int. Ed.* **2023**, *62*, No. e202303966. (f) Rodríguez-Salamanca, P.; Fernández, R.; Hornillos, V.; Lassaletta, J. M. Asymmetric Synthesis of Axially Chiral C−N Atropisomers. *Chem.—Eur. J.* **2022**, *28*, No. e202104442. (g) Mei, G.-J.; Wong, J. J.; Zheng, W.; Nangia, A. A.; Houk, K. N.; Lu, Y. Rational Design and Atroposelective Synthesis of N−N Axially Chiral Compounds. *Chem.* **2021**, *7*, 2743−2757. (h) Kitagawa, O. Chiral Pd-Catalyzed Enantioselective Syntheses of Various N−C Axially Chiral Compounds and Their Synthetic Applications. *Acc. Chem. Res.* **2021**, *54*, 719−730.

(13) For selected reviews, see: (a) Li, Y.; Lu, X.; Fu, Y. Recent Advances in Cobalt-Catalyzed Regio- or Stereoselective Hydrofunctionalization of Alkenes and Alkynes. *CCS Chem.* **2024**, *6*, 1130−1156. (b) Dong, B.; Shen, J.; Xie, L.-G. Recent Developments on 1,2-Difunctionalization and Hydrofunctionalization of Unactivated Alkenes and Alkynes Involving C−S Bond Formation. *Org. Chem. Front.* **2023**, *10*, 1322−1345. (c) Guo, J.; Cheng, Z.; Chen, J.; Chen, X.; Lu, Z. Iron- and Cobalt-Catalyzed Asymmetric Hydrofunctionalization of Alkenes and Alkynes. *Acc. Chem. Res.* **2021**, *54*, 2701−2716. (d) Zhang, Z.-X.; Zhai, T.-Y.; Ye, L.-W. Synthesis of Axially Chiral Compounds Through Catalytic Asymmetric Reactions of Alkynes. *Chem. Catal.* **2021**, *1*, 1378−1412. (e) Li, G.; Huo, X.; Jiang, X.; Zhang, W. B. Asymmetric Synthesis of Allylic Compounds via Hydrofunctionalisation and Difunctionalisation of Dienes, Allenes, and Alkynes. *Chem. Soc. Rev.* **2020**, *49*, 2060−2118. (f) Cheng, Z.; Guo, J.; Lu, Z. Recent Advances in Metal-Catalysed Asymmetric Sequential Double Hydrofunctionalization of Alkynes. *Chem. Commun.* **2020**, *56*, 2229−2239.

(14) Jia, S.; Chen, Z.; Zhang, N.; Tan, Y.; Liu, Y.; Deng, J.; Yan, H. Organocatalytic Enantioselective Construction of Axially Chiral Sulfone-Containing Styrenes. *J. Am. Chem. Soc.* **2018**, *140*, 7056−7060.

(15) Wang, Y.-B.; Yu, P.; Zhou, Z.-P.; Zhang, J.; Wang, J.; Luo, S.-H.; Gu, Q.-S.; Houk, K. N.; Tan, B. Rational Design, Enantioselective Synthesis and Catalytic Applications of Axially Chiral EBINOLs. *Nat. Catal.* **2019**, *2*, 504−513.

(16) (a) Ji, D.; Jing, J.; Wang, Y.; Qi, Z.; Wang, F.; Zhang, X.; Wang, Y.; Li, X. Palladium-Catalyzed Asymmetric Hydrophosphination of Internal Alkynes: Atroposelective Access to Phosphine-Functionalized Olefins. *Chem.* **2022**, *8*, 3346. (b) Cai, B.; Cui, Y.; Zhou, J.; Wang, Y.-B.; Yang, L.; Tan, B.; Wang, J. Asymmetric Hydrophosphinylation of Alkynes: Facile Access to Axially Chiral Styrene-Phosphines. *Angew. Chem., Int. Ed.* **2023**, *62*, No. e202215820.

(17) Sheng, F.-T.; Wang, S.-C.; Zhou, J.; Chen, C.; Wang, Y.; Zhu, S. Control of Axial Chirality Through NiH-Catalyzed Atroposelective Hydrofunctionalization of Alkynes. *ACS Catal.* **2023**, *13*, 3841−3846.

(18) Ma, X.; Tan, M.; Li, L.; Zhong, Z.; Li, P.; Liang, J.; Song, Q. Ni-Catalysed Assembly of Axially Chiral Alkenes from Alkynyl Tetracoordinate Borons via 1,3-Metallate Shift. *Nat. Chem.* **2024**, *16*, 42−53.

(19) Zhan, L.-W.; Lu, C.-J.; Feng, J.; Liu, R.-R. Atroposelective Synthesis of C−N Vinylindole Atropisomers by Palladium-Catalyzed Asymmetric Hydroarylation of 1-Alkynylindoles. *Angew. Chem., Int. Ed.* **2023**, *62*, No. e202312930.

(20) Wu, Q.; Zhang, Q.; Yin, S.; Lin, A.; Gao, S.; Yao, H. Atroposelective Synthesis of Axially Chiral Styrenes by Platinum-Catalyzed Stereoselective Hydrosilylation of Internal Alkynes. *Angew. Chem., Int. Ed.* **2023**, *62*, No. e202305518.

(21) (a) Neto, J. S. S.; Zeni, G. Recent Advances in the Synthesis of Indoles from Alkynes and Nitrogen Sources. *Org. Chem. Front.* **2020**, *7*, 155−210. (b) Karamyan, A. J. K.; Hamann, M. T. Marine Indole Alkaloids: Potential New Drug Leads for the Control of Depression and Anxiety. *Chem. Rev.* **2010**, *110*, 4489−4497.

(22) Zhu, X.; Mi, R.; Yin, J.; Wang, F.; Li, X. Rhodium-Catalyzed Atroposelective Access to Trisubstituted Olefins via C−H Bond Olefination of Diverse Arenes. *Chem. Sci.* **2023**, *14*, 7999−8005.

https://doi.org/10.1021/acscatal.4c03710
ACS Catal. 2024, 14, 13055−13064